High Verdet constant of $Te_{20}As_{30}Se_{50}$ glass in the mid-infrared

Masoud Mollaee,[1] Pierre Lucas,[2] Julien Ari[2], Xiushan Zhu,[1,*] Michal Lukowski,[1] Tariq Manzur[1] and N. Peyghambarian[1]

[1]*College of Optical Sciences, the University of Arizona, Tucson, AZ, 85721, USA*
[2]*Department of Material Sciences and Engineering, the University of Arizona, Tucson, AZ, 85719, USA*

**Corresponding author: xszhu@email.arizona.edu*

Received XX Month XXXX; revised XX Month, XXXX; accepted XX Month XXXX; posted XX Month XXXX (Doc. ID XXXXX); published XX Month XXXX

Magneto optical properties of tellurium-arsenic-selenium glass ($Te_{20}As_{30}Se_{50}$) were measured and analyzed. A Verdet constant of 15.18 rad/T/m at 1950 nm with the figure of merit of more than 8.72 rad/T, which is the highest value reported in glass materials at this wavelength, was measured. Compared to other chalcogenide glasses, such as $Ge_{10}Se_{90}$ and $Ge_{25}As_{15}S_{60}$, $Te_{20}As_{30}Se_{50}$ glass exhibits higher Verdet constants, broader mid-infrared transparency window, and longer infrared absorption edge, making it a very promising material to fabricate magneto-optical devices for mid-infrared applications.

OCIS codes: *(160.3820) Magneto-optical materials; (230.2240) Faraday effect; (160.2750) Glass and other amorphous materials; (160.3380) Laser materials.*

Magneto-Optical (MO) materials have attracted a lot of attention due to their extensive applications in optical switches, isolators, circulators, modulators, security encoding and sensing components[1–3]. In particular, optical isolators and circulators are highly needed in optical systems to protect upstream devices from the influence of the backward propagated light or force the light to propagate unidirectionally [4]. The operation of optical isolators or circulators are based on the Faraday rotation effect of MO materials, which causes the rotation of the polarization plane of the light by the magnetic field and is quantified by the Verdet constant (V). Ytterium iorn garnet (YIG) and terbium gallium garnet (TGG) are the most common materials used for different MO applications, owing to their high Verdet constant and low loss [1, 5]. But these materials are sensitive to temperature, and since they are usually used in cystal form, they cannot be used for applications where isotropic MO property is required or MO devices with extreme sizes are needed. Compared to crystals, glasses have the advantages of isotropy, easy fabrication, low cost, and can be made into devices with complicated shapes and extreme sizes. Therefore, MO glasses have been extensively studied over the past decades. But most studies were conducted in the visible and near infrared (IR) wavelength regions [3, 6, 7]. Due to the rapid development of mid-IR technologies, there is a great demand for mid-IR MO glasses. In this paper, we present our study of the MO properties of tellurium-arsenic-selenium glass ($Te_{20}As_{30}Se_{50}$) and a Verdet constant measureemnt of 15.18 rad/T/m at 1950 nm, which is the highest value reported in glass material at this wavelength, to the best of our knowledge.

Generally, MO materials can be categorized into diamagnetic materials and paramagnetic materials. Rare-earth doped glasses are paramagnetic materials, which are highly temperature dependent[8] and thus cannot work steadily and consistently in a harsh environment. High Verdet constant of a paramagnetic glass can generally be achieved with increasing the doping concentration of rare-earth elements. But it also leads to deterioration in the chemical stability and optical transmittance. Undoped glasses are diamagnetic materials, which usually have a very low temperature dependence [8]. Oxide glasses have been extensively used in the visible and near-infrared (IR) wavelength regions and their MO properties have also been studied [9, 10]. However, the Verdet constants of oxide glasses are usually low. For example, silica glass has a Verdet constant of 1 rad/T/m in 1064 nm[7] and even for zinc-tellurite glass, V is about 9.94 rad/T/m at 1 μm[11]. Moreover, the short multi-phonon IR absorption of most oxide glasses also limit their applications in the mid-IR. Compared to oxide glasses, chalcogenide glasses have much longer multi-phonon IR absorption edge and have been made into optical components and optical fibers for a variety of mid-IR applications. Due to their large refractive index dispersion, chalcogenide glasses also exhibit attractive MO properties. For instance, the Verdet constant of $Ge_{33}As_{12}Se_{55}$ was measured to be 14.06 rad/T/m at 1550 nm and that of $75GeS_2{\cdot}25Ga_2S_3$ was measured to be 14.50 rad/T/m at 1340 nm [12, 13]. Both of them are much larger than that of zinc-tellurite

glass at the two wavelengths. By incorporating some large atoms to increase the polarizibility, *V*erdet constants of about 20.93 rad/T/m and 18.84 rad/T/m at 1319 nm were measured in $60GeS_2{\cdot}15In_2S_3{\cdot}25PbI_2$, and $80GeS_220Sb_2S_3$, respectivley [14, 15]. Therefore, a chalcogenide glass with improved MO properties in the mid-IR may be sythesized by introducing large atoms that can lead to high polarizability and long absorption edges.

Here, we present the MO properties of $Te_{20}As_{30}Se_{50}$, which has a multi-phonon IR absorption edge of 18 μm and a bandgap short-wavelength absorption edge of 1200 nm. Compared to the other chalcogenide glasses, such as $Ge_{10}Se_{90}$, and $Ge_{25}As_{15}S_{60}$, $Te_{20}As_{30}Se_{50}$ glass has much higher Verdet constant at near-IR and mid-IR wavelength due to its smaller electronic bandgap. Verdet constants of 22.68 rad/T/m and 15.18 rad/T/m were measured at 1555 nm and 1950 nm, respectively, which are the highest reported Verdet constants of diamagnetic materials in the mid-IR, to the best of our knowledge. The Figure of Merit (FOM) of the the $Te_{20}As_{30}Se_{50}$ was measured to be more than 500 rad/T at 1950 nm, which makes it a promising material for MO applications.

$Te_{20}As_{30}S_{50}$ glass was selected as a promising MO diamagnetic glass for mid-IR because it has a long IR absorption edge, large refractive index dispersion, and high chemical stability [10]. Two technologically relevant chalcogenide glasses, $Ge_{10}Se_{90}$, and $Ge_{25}As_{15}S_{60}$, which have MO properties similar to the previous reports were also fabricated for comparison in our experiment. Three chalcogenide glass samples were synthesized by the melting quench method starting from high purity raw elements Ge (5N), As (6N), S (5N), Se (5N) and Te (5N). Stoichiometric amounts of different glass compositions were weighed in a glove box under argon and introduced in silica tube under vacuum (10^{-6} mbar) before sealing the ampoules. The melts were homogenized in a rocking furnace for 10 hours between 800°C–850°C and the temperature was subsequently lowered to 600-650°C in 2 hours before quenching the ampoules in water at room temperature. The ampoules were then readily introduced in an annealing oven preheated at 10°C below the glass transition temperature (Tg) for 5 hours, then the ampoules were slowly cooled down to room temperature at 0.5°C/min.

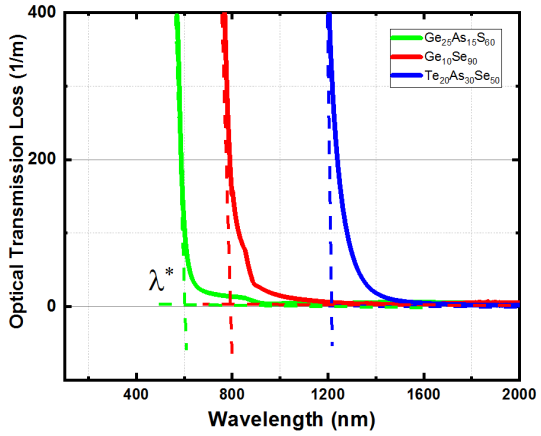

Fig. 1: Optical transmission loss spectra of $Te_{20}As_{30}Se_{50}$, $Ge_{10}Se_{90}$, and $Ge_{25}As_{15}S_{60}$. The crossing point of two dashed lines show the bandgap absorption edge.

The optical near-IR and IR transmision of the three glasses were measured at room temperature using a Cary 5000 UV-Vis-NIR Spectrometer and a Bruker Tensor 27 FTIR spectrometer, respectively. Fig. 1 shows the optical transmission loss spectra of $Te_{20}As_{30}Se_{50}$, $Ge_{10}Se_{90}$, and $Ge_{25}As_{15}S_{60}$, which were calculated from the measured optical transmission spectra of the glass samples with different lengths. All three glasses have a low absorption in the region near 2 μm. The bandgap absorption edge, λ*, of a glass is related to the energy gap between the valence band and the conduction band and is determined by the crossing point of the two tangent dashed lines, as shown in Fig. 1. The bandgap absorption edges of $Te_{20}As_{30}Se_{50}$, $Ge_{10}Se_{90}$, and $Ge_{25}As_{15}S_{60}$ were found to be 1200, 780, and 592 nm, respectively. Clearly, $Te_{20}As_{30}Se_{50}$ glass has a much longer bandgap absorption edge than $Ge_{10}Se_{90}$, and $Ge_{25}As_{15}S_{60}$ due to the large tellurium atom.

Fig. 2 shows the IR transmission spectra of all three glasses from 1 μm to 20 μm. The transparency window of $Te_{20}As_{30}Se_{50}$ is extended up to 18 μm, while that of $Ge_{10}Se_{90}$ and $Ge_{25}As_{15}S_{60}$ is only extended up to 16 μm and 11 μm, respectively. The longer IR absorption edge of $Te_{20}As_{30}Se_{50}$ is due to the heavy atom of tellurium.

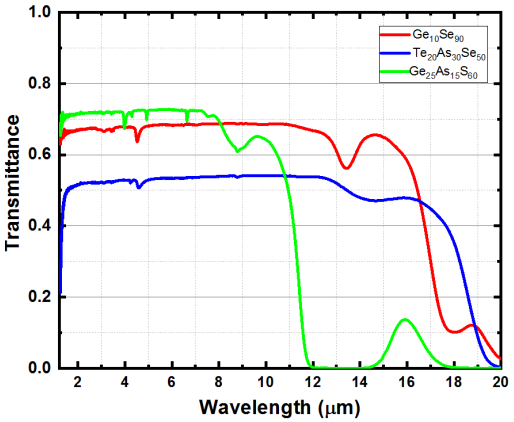

Fig. 2: IR transmission spectra of $Te_{20}As_{30}Se_{50}$, $Ge_{10}Se_{90}$, and $Ge_{25}As_{15}S_{60}$.

The Verdet constants of the three glass samples were measured at room temperature, using the experimental setup depicted in Fig. 3, which consists of a light source, a Glan-Thompson (GT) polarizer, an achromatic half wave plate, a solenoid, a Wollaston polarizer, and two photodetectors to measure the power of the S-polarized and P-polarized light. Linearly polarized light with a polarization extinction ratio of more 30 dB is achieved with a GT polarizer. The plane of the polarized light can be ajusted by a half-wave (λ/2) plate so that it is at an angle of 45° as the light goes throught the MO glass in the absence of a magnetic field and arrives at the Wollaston polarizer, which can separate the S and P polarized light equally. When a magnetic field is applied to the MO glass by the solenoid, the plane of the polarzied light rotates. The rotation angle can be calculated from the power of S and P polarized light measured by the two photodectors. The measurement resolution of the setup for Faraday rotation was higher than 0.01°. The Verdet constant can be calculated from the change in rotation angle of the linearly polarized light, the applied magnetic field, and the glass length with following equation .

$$V = \frac{\theta}{BL} \quad (1)$$

Where, θ is the angle of the linearly polarized light rotated by the solenoid, B is the magnetic flux of the solenoid, and L is the glass length.

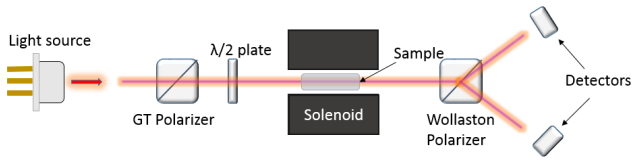

Fig. 3: The schematic setup for Verdet constant measurement.

The Verdet constants of the three glasses were measured at 1240, 1476, 1555, and 1950 nm and are shown in Fig. 4. Clearly, compared to $Ge_{25}As_{15}S_{60}$, and $Ge_{10}Se_{90}$ glasses, $Te_{20}As_{30}Se_{50}$ glass has much larger Verdet constant due to the longer bandgap absorption edge. Based on the model of single oscillator with a narrow band resonance wavelength, the wavelength dependence of Verdet constant can be written as a simplified *Borrelli* equation as [8]

$$V = \frac{C\lambda^2}{\left(1-\frac{\lambda^2}{\lambda_0^2}\right)^2} \quad (2)$$

Where V, λ, and λ_0 are the Verdet constant, the wavelength of the light, and the average resonant wavelength of the material, respectively. C is a wavelength independent constant that includes the Landé factor, the velocity of light, the Planck constant, and the effective transition probability.

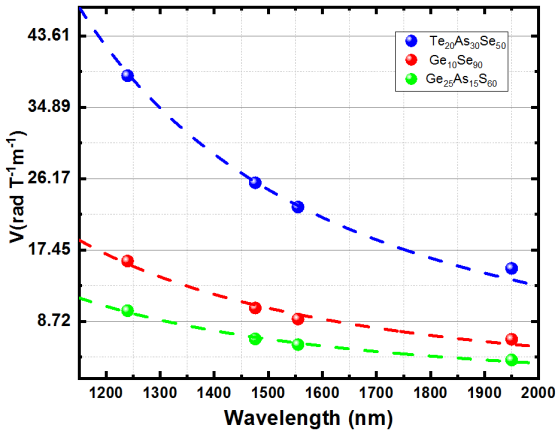

Fig. 4: Verdet constants of $Te_{20}As_{30}Se_{50}$, $Ge_{10}Se_{90}$, and $Ge_{25}As_{15}S_{60}$ measured at 1240, 1476, 1555, and 1950 nm. The dashed lines are the fitting curves.

The C and λ_0 for each glass can be found by fitting the experimental results with equation (2) as shown by the dashed curves in Fig. 4. The C and λ_0 of $Te_{20}As_{30}Se_{50}$ were found to be 0.0019 rad·T^{-1}·m^{-1}·nm^{-2} and 400 nm, respectively. For $Ge_{10}Se_{90}$, C and λ_0 were found to be 0.0026 rad·T^{-1}·m^{-1}·nm^{-2} and 300 nm, respectively. For $Ge_{25}As_{15}S_{60}$, C and λ_0 were found to be 0.0036 rad·T^{-1}·m^{-1}·nm^{-2} and 250 nm, respectively. Because the average resonance wavelength of $Te_{20}As_{30}Se_{50}$ is longer than that of $Ge_{25}As_{15}S_{60}$, and $Ge_{10}Se_{90}$, a Verdet constant of 15.18 rad/T/m at 1950 nm is much larger than 4 rad/T/m and 6.52 rad/T/m of two germanium-based chalcogenide glasses. It is also the highest Verdet constant of glass materials that has been reported in the 2μm region, to the best of our knowledge.

Several previous studies have shown that the Verdet constants of diamagnetic glasses at $\lambda >> \lambda_0$ always increase with the increased bandgap absorption edge [12,15]. This can be verified by our experimental data. The measured Verdet constants of $Te_{20}As_{30}Se_{50}$, $Ge_{25}As_{15}S_{60}$, and $Ge_{10}Se_{90}$ glasses measured at 1240, 1476, 1555, and 1950 nm were plotted versus the squared bandgap absorption edge and are shown in Fig. 5. All the measurement data at the four wavelengths can be fitted with linear curves, indicating that the Verdet constant is approximately proportional to λ^{*2}, which is in agreement with previous observation reported by Qiu et al. [16]. Therefore, synthesizing diamagnetic glass with a long bandgap absorption edge is an effective method to achieve a high Verdet constant in the mid-IR.

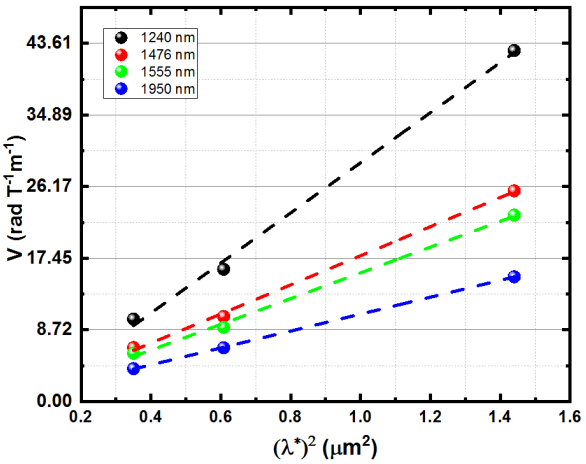

Fig. 5: Verdet constants of $Te_{20}As_{30}Se_{50}$, $Ge_{10}Se_{90}$, and $Ge_{25}As_{15}S_{60}$ were plotted at the λ^{*2} for the light wavelengths of 1240, 1476, 1555, and 1950 nm.

The absolute value of Verdet constants of different materials operating in 2 μm region is tabulated in Table 1. As it can be seen the Verdet constant of $Te_{20}As_{30}Se_{50}$ glass is higher than $(Dy_{0.9}Y_{0.05}La_{0.05})_2O_3$ ceramic. It should be noted the operation range of chalcogenide glasses are significantly brother than Dy doped ceramics.

Table 1: Verdet constant of differet materials operating in 2 μm region.

Materials	Type	V (rad/T/m)	λ (nm)
YIG [17]	Crystal	350	1960
$(Dy_{0.9}Y_{0.05}La_{0.05})_2O_3$ [18]	Ceramic	13.8	1940
$Te_{20}As_{30}Se_{50}$	Glass	15.18	1950
$60GeS_2{\cdot}15In_2S_3{\cdot}25PbI_2$ [14]	Glass	20.93	1319
$Ge_{10}Se_{90}$	Glass	6.52	1950

In addition to large Verdet constant, very low loss is also a desired feature of a MO material. The performance of a MO material is usually evaluated by FOM, which is defined as:

$$FOM = \frac{V}{\alpha} \quad (3)$$

Where V and α is the Verdet constant and optical transmission loss, respectively. FOM of all three glasses were calculated with measured optical transmission loss and the Verdet constants shown in Fig. 4 and are shown in Fig. 6. It is clear that the FOM of $Te_{20}As_{30}Se_{50}$ is significantly higher than that of the other two glasses at 1700 - 2100 nm, indicating that $Te_{20}As_{30}Se_{50}$ is a very promising diamagentic material for MO applications in the 2 μm wavelength region. Similar to the general feature of FOM for other materials, the FOM of $Te_{20}As_{30}Se_{50}$ is very small at short wavelengths close to the bandgap absorption edge due to the large absorption. Because the bandgap absorption always decreases with the increasing wavelength in undoped glasses, the FOM increases as the wavelength goes to longer wavelengths. A maximum FOM of 8.72 rad/T is obtained at 1905 nm because the Verdet constant also decreases with the increasing wavelength as shown in Fig. 4. The FOM beyond 1905 nm decreases with the increasing wavelength because the Verdet constant decreases more rapidly than the optical transmission loss. The FOM of $Ge_{10}Se_{90}$ exhibits similar features and has a maximum value of 3.70 rad/T around 1440 nm. Because the bandgap absorption edges of $Ge_{25}As_{15}S_{60}$ is 592 nm, which is far from the measurement range of 1200-2100 nm, the FOM continuously decreases with the increasing wavelength.

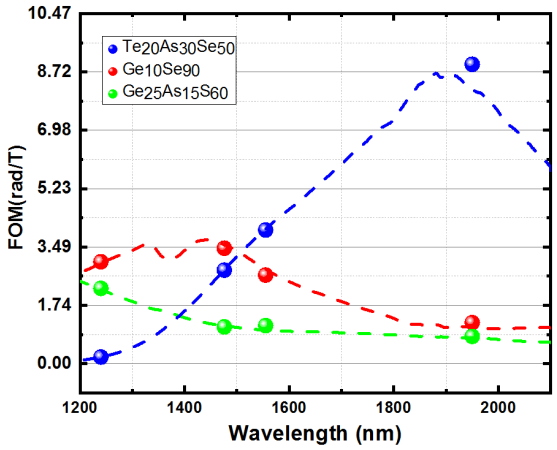

Fig. 6: FOMs of $Te_{20}As_{30}Se_{50}$, $Ge_{25}As_{15}S_{60}$, and $Ge_{10}Se_{90}$ glasses as a function of the wavelength. The solid dots show the measured FOM.

In conclusion, $Te_{20}As_{30}Se_{50}$ glass was fabricated and its MO properties were measured and analyzed. The bandgap absorption edge and IR multi-phonon absorption edge of $Te_{20}As_{30}Se_{50}$ glass were measured to be 1200 nm and 18 μm, respectively. The Verdet constants at 1555 nm and 1950 nm were measured to be 22.68 rad/T/m and 15.18 rad/T/m, which are much larger than other chalcogenide glasses. The FOM was found to be more than 6.98 rad/T at the 2 μm wavelength region. All these results show that $Te_{20}As_{30}Se_{50}$ glass is a very promising MO material with low temperature dependence for mid-IR applications.

Funding. This work was supported by Technology Research Initiative Fund (TRIF) Photonics Initiative of University of Arizona and NSF-DMR under grant#: 1832817

Disclosures. The authors declare no conflicts of interest.

1. G. Bendelli, S. Donati, E. Universita, and V. Abbiategrasso, Opt. Commun. **3**, 373 (1992).
2. L. Sun, S. Jiang, and J. R. Marciante, Opt. Express **18**(6), 5407 (2010).
3. Y. Huang, H. Chen, W. Dong, F. Pang, J. Wen, Z. Chen, and T. Wang, Opt. Express **24**(16), 181 (2016).
4. H. Dötsch, N. Bahlmann, O. Zhuromskyy, M. Hammer, L. Wilkens, R. Gerhardt, P. Hertel, and A. F. Popkov, J. Opt. Soc. Am. B **22**, 240 (2005).
5. I. L. Snetkov, A. V. Voitovich, O. V. Palashov, and E. A. Khazanov, IEEE J. Quantum Electron. **50**, 434 (2014).
6. R. Yasuhara, S. Tokita, J. Kawanaka, and et. al., Opt. Express **15**(18), 11255 (2007).
7. L. Sun, S. Jiang, J. D. Zuegel, and J. R. Marciante, Opt. Lett. **34**(11), 1699 (2009).
8. W. A. Crossley, R. W. Copper, and J. L. Page, Phys. Rev. **181**, 896 (1969).
9. N. F. Borrelli, J. Chem. Phys **41**, 3289 (1964).
10. N. V Ovcharenko and T. V Smirnova, J. Non-Crystalline Solids Cryst. Solids **291**, 121 (2001).
11. A. I. Yakovlev, I. L. Snetkov, V. V. Dorofeev, and S. E. Motorin, J. Non. Cryst. Solids **480**, 90 (2018).
12. Y. Ruan, R. A. Jarvis, A. V Rode, S. Madden, and B. Luther-Davies, Opt. Commun. **252**, 39 (2005).
13. X. Xiao, X. Cui, F. Gao, J. Cui, X. Liu, H. Guo, J. She, G. Chen, B. Peng, C. J. Firby, A. Y. Elezzabi, H. Dötsch, N. Bahlmann, O. Zhuromskyy, M. Hammer, L. Wilkens, R. Gerhardt, P. Hertel, and A. F. Popkov, Opt. Mater. Express **8**, 1754 (2018).
14. Y. Xu, H. Guo, X. Xiao, P. Wang, X. Cui, M. Lu, C. Lin, S. Dai, and B. O. Peng, Opt. Express **25**, 20410 (2017).
15. G. Chen, Y. Xu, H. Guo, X. Cui, P. Wang, M. Lu, X. Xiao, Q. Guo, and B. Peng, J. Am. Ceram. Soc. **100**, 2914 (2017).
16. J. Qiu and K. Hirao, J. Mater. Res. **13**, 1358 (1998).
17. G. Stevens, T. H. Legg, and P. Shardlow, in Proc. SPIE 9346, Components and Packaging for Laser Systems, **9346** (2015).
18. I. L. Snetkov, A. I. Yakovlev, D. A. Permin, S. S. Balabanov, and O. V Palashov, Opt. Lett. **43**, 4041 (2018).

1. G. Bendelli, S. Donati, E. Universita, and V. Abbiategrasso, "Optical Isolators for Telecommunications: Review and Current Trends," Opt. Commun. **3**, 373–380 (1992).
2. L. Sun, S. Jiang, and J. R. Marciante, "All-fiber optical magnetic-field sensor based on Faraday rotation in highly terbium-doped fiber," Opt. Express **18**(6), 5407-5412 (2010).
3. Y. Huang, H. Chen, W. Dong, F. Pang, J. Wen, Z. Chen, and T. Wang, "Fabrication of europium-doped silica optical fiber with high Verdet constant," Opt. Express **24**(16), 181–189 (2016).
4. H. Dötsch, N. Bahlmann, O. Zhuromskyy, M. Hammer, L. Wilkens, R. Gerhardt, P. Hertel, and A. F. Popkov, "Applications of magneto-optical waveguides in integrated optics: review," J. Opt. Soc. Am. B **22**, 240–253 (2005).
5. I. L. Snetkov, A. V. Voitovich, O. V. Palashov, and E. A. Khazanov, "Review of faraday isolators for kilowatt average power lasers," IEEE J. Quantum Electron. **50**, 434-443 (2014).
6. R. Yasuhara, S. Tokita, J. Kawanaka, and E. Al., "Cryogenic temperature characteristics of Verdet constant on terbium gallium garnet ceramics," Opt. Express **15**(18), 11255-11261 (2007).
7. L. Sun, S. Jiang, J. D. Zuegel, and J. R. Marciante, "Effective Verdet constant in a terbium-doped-core phosphate fiber," Opt. Lett. **34**(11), 1699–1701 (2009).
8. W. A. Crossley, R. W. Copper, and J. L. Page, "Faraday Rotation in Rare-Earth Iron Garnets," Phys. Rev. **181**, 896–904 (1969).
9. N. F. Borrelli, "Faraday Rotation in Glasses," J. Chem. Phys **41**, 3289-3293 (1964).
10. N. V Ovcharenko, and T. V Smirnova, "High refractive index and magneto-optical glasses in the systems TeO_2-WO_3-Bi_2O_3 and TeO_2-WO_3-PbO," J. Non-Crystalline Solids Cryst. Solids **291**, 121–126 (2001).
11. A. I. Yakovlev, I. L. Snetkov, V. V. Dorofeev, and S. E. Motorin, "Magneto-optical properties of high-purity zinc-tellurite glasses," J. Non. Cryst. Solids **480**, 90–94 (2018).
12. Y. Ruan, R. A. Jarvis, A. V Rode, S. Madden, and B. Luther-Davies, "Wavelength dispersion of Verdet constants in chalcogenide glasses for magneto-optical waveguide devices," Opt. Commun. **252**, 39-45 (2005).
13. X. Xiao, X. Cui, F. Gao, J. Cui, X. Liu, H. Guo, J. She, G. Chen, B. Peng, C. J. Firby, A. Y. Elezzabi, H. Dötsch, N. Bahlmann, O. Zhuromskyy, M. Hammer, L. Wilkens, R. Gerhardt, P. Hertel, and A. F. Popkov, "Improvement of the Faraday effect in Ge-S based chalcogenide glasses via gallium and lead compositional modifications," Opt. Mater. Express **8**(7), 1754 (2018).
14. Y. Xu, H. Guo, X. Xiao, P. Wang, X. Cui, M. Lu, C. Lin, S. Dai, and B. O. Peng, "High Verdet constants and diamagnetic responses of GeS_2-In_2S_3-PbI_2 chalcogenide glasses for integrated optics applications," Opt. Express **25**, 20410-20420 (2017).
15. G. Chen, Y. Xu, H. Guo, X. Cui, P. Wang, M. Lu, X. Xiao, Q. Guo, and B. Peng, "Magneto-optical effects of Ge-Ga-Sb(In)-S chalcogenide glasses with diamagnetic responses," J. Am. Ceram. Soc. **100**, 2914-2920 (2017).
16. J. Qiu and K. Hirao, "The Faraday effect in diamagnetic glasses," J. Mater. Res. **13**, 1358-1362 (1998).
17. G. Stevens, T. H. Legg, and P. Shardlow, "Optical isolators for 2-micron fibre lasers," in Proc. SPIE 9346, Components and Packaging for Laser Systems, **9346**, 1-6 (2015).
18. I. L. Snetkov, A. I. Yakovlev, D. A. Permin, S. S. Balabanov, and O. V Palashov, "Magneto-optical Faraday effect in dysprosium oxide (Dy_2O_3) based ceramics obtained by vacuum sintering," Opt. Lett. **43**, 4041-4044 (2018).